ISBN: 978-3-95450-261-5 ISSN: 2673-7000 doi: 10.18429/JACoW-NAPAC2025-MOP093

TOWARDS ACCURATE BEAM SIGMA MATRIX DETERMINATION IN A TRANSPORT LINE USING DIFFERENTIABLE SIMULATION*

C. Xu†, M. Borland, L. Emery, O. Mohsen, Y. Sun, Argonne National Laboratory, Lemont, IL, USA
R. Roussel, SLAC National Accelerator Laboratory, Menlo Park, CA, USA

Abstract

Precise characterization of the beam distribution is essential for matching the incoming beam and optimizing injection into storage rings. We present a method to efficiently reconstruct the full 5×5 beam sigma matrix (excluding the time coordinates) at the booster-to-storage-ring (BTS) transport line at the Advanced Photon Source Upgrade (APS-U). Earlier works demonstrated that the beam sigma matrix can be accurately reconstructed using linear transport matrices under the assumption of negligible chromatic effects. However, the presence of chromaticity introduced significant non-linearities and leads to discrepancies from the linear approaches. In this work, we demonstrate a novel approach leveraging Cheetah, a differentiable beam dynamics simulation framework, to enable direct gradient-based optimization of the beam matrix. Initial results shows efficient and accurate reconstruction under both linear and second-order tracking models, providing improved robustness in simulation studies. This method offers a scalable, interpretable, and computationally efficient alternative to black-box methods for beam matrix reconstruction in transport lines in presence of complex effects.

INTRODUCTION

A standard method for characterizing the beam properties in a transport line is the quadrupole scan. By varying the strengths of multiple quadrupoles and observing the transverse beam sizes on a downstream screen, we could measure the emittances or the transverse 4×4 beam sigma matrix [1]. When the quadrupole magnets are placed at locations with non-zero dispersion, the resulted transverse beam profile further depends on the beam momentum. As such, it allows the determination of 5×5 beam sigma matrix, excluding the temporal part. Relying on the linear transport matrices, the output beam moments can be expressed as a linear equation system of the initial beam sigma matrix, which can be solved to obtain the incoming beam properties [2, 3]. While this method works well for linear systems, the discrepancies increase when the system cannot be sufficiently approximated by first order transport matrices, for example due to strong chromatic effects. As a result, the linear solution needs to be further adjusted to accurately determine the beam properties. This can be achieved using black box optimization methods like genetic algorithms. However, as the problem has high-dimensionality and is non-convex, the fitting requires many sample evaluations, often taking hours. In recent years, several differentiable beam dynamics simulation codes were developed, including the PyTorch-based package Cheetah [4, 5], Bmad-Julia [6], and JuTrack [7]. They utilize the auto-differentiation (AD) technique which allow automatic calculation of derivatives alongside of the particle tracking. In this paper, we describe using Cheetah for gradient-based optimization of the initial 5×5 beam sigma matrix. This approach resembles the generative phase space reconstruction (GPSR) [8, 9] method, which leverages differentiable simulation to reconstruct the 6-dimensional phase space distribution from a small number of transverse beam images by scanning quadrupoles, a transverse-deflecting cavity, and a dipole spectrometer.

* The work is supported by the U.S. DOE Office of Science-Basic Energy Sciences, under Contract No. DE-AC02-06CH11357.
† chenran.xu@anl.gov

GRADIENT-BASED OPTIMIZATION OF BEAM SIGMA MATRIX

We start with the initial particles $\boldsymbol{x}_0 = (x, p_x, y, p_y, \tau, \delta)$ distributed according to the design settings. The unknown beam distribution at the entrance of the transport line is represented by a matrix which transforms the initial particles by

$$\boldsymbol{x}_t = \boldsymbol{x}_0 R_{\boldsymbol{\theta}}^T, \tag{1}$$

with $\{R_{ij}, i, j \neq 5\}$ being the non-temporal components to be determined. The transformed particles $\boldsymbol{x}_t$ are further tracked through the transport line up to second order with the transfer function

$$\boldsymbol{x}_f = f(\boldsymbol{x}_t | \boldsymbol{k}_Q), \tag{2}$$

which depends on the quadrupole strengths $\boldsymbol{k}_Q = (k_{Q_1}, \ldots, k_{Q_j})$. The screen images are simulated from the phase space coordinates of the output macroparticles using the kernel density estimation (KDE) method, allowing the gradients to be propagated $Y_f = \mathrm{KDE}(\boldsymbol{x}_f)$. By evaluating different quadrupole settings $\boldsymbol{k}_Q^{1,\ldots,n}$, a set of n screen images are generated. A loss function can be calculated between the simulated and target screen images

$$l = \sum_{i=1,\ldots,n} \mathrm{Loss}(Y_f^i - Y_{\mathrm{target}}^i). \tag{3}$$

As such, the goal is to minimize the differences between the simulated and the target images by finding the best initial transform matrix

$$\min_{\boldsymbol{\theta}} l(Y_{\mathrm{target}}, Y_f(\boldsymbol{\theta})), \ \boldsymbol{\theta} \in \mathbb{R}^{5\times5}. \tag{4}$$

When tracking the particles with a differentiable simulation code such as Cheetah [4], we automatically obtain the gradient of the loss function with respect to the unknown

ISBN: 978-3-95450-261-5 ISSN: 2673-7000 doi: 10.18429/JACoW-NAPAC2025-MOP093

transform matrix $\boldsymbol{\theta}$ and use gradient-descent to update the parameters. This approach can be easily customized to include further components or differentiable physical effects in the tracking, as long as the gradient propagation is preserved. To handle beam distributions with complex structures, the initial transformation can be also extended beyond a simple linear matrix $R_{\boldsymbol{\theta}}$ to other functions, or even a fully-connected neural network (NN) as in the case of GPSR.

SIMULATED STUDY

First, we demonstrate the method in simulation on the new BTS transport line at APS-U [10]. The new design includes stronger quadrupole and leads to more pronounced chromatic effects compared to the old one. Figure 1 shows part of the BTS lattice until the diagnostic screen FS3. Three quadrupoles (AQ4, AQ5, and BQ1) are used for scanning, with the first two having non-zero dispersions. The quadrupoles are denoted by vertical lines in the figure. In total, 30 quadrupole settings are chosen as described in the earlier work [2]. These settings are expected to have full transmission and reasonable beam sizes at the diagnostic screen. In simulation, we randomly vary the initial sigma matrix by adding a 5% error drawn from a normal distribution. The reconstruction is repeated 5 times to estimate the uncertainty of the beam parameters, starting from slightly different initial conditions. The results are listed in Table 1. The method is able to correctly reconstruct most parameters within the uncertainty range. In the horizontal-plane, there seems to be a systematic underestimation of a few percents.

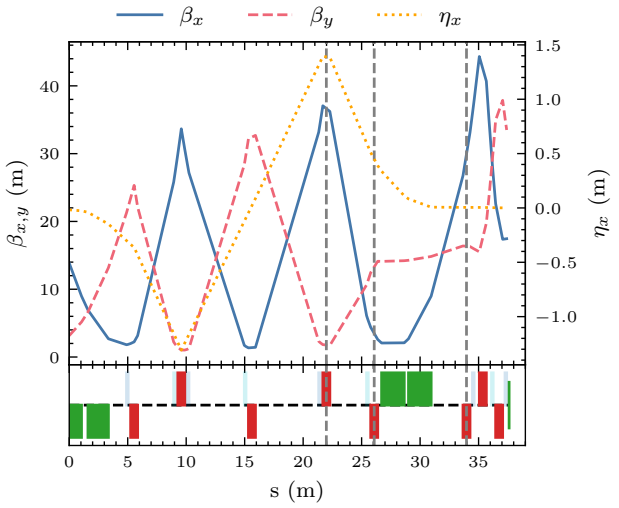

Figure 1: Lattice of the BTS transport line until the diagnostic screen FS3. The three vertical lines denote the positions of the quadrupoles (AQ4, AQ5, and BQ1) that are being varied for the beam matrix measurement.

REAL-WORLD MEASUREMENT

Next, we conducted actual measurement to test the applicability of the method. For each set of quadrupole settings, 10 subsequent beam images on the diagnostic screen were taken. Background images are subtracted from the measured images, and the hot pixels were removed. As the trajectory control was not running during the measurement, the beam was observed to move over the screen due to the beam offset relative to the quadrupole magnets. The quadrupole offset could potentially be determined simultaneously given enough measured images. The beam offsets also introduced fixed and variable dispersions for fixed and variable quadrupoles respectively [2], which is not included in the model but can be addressed using the BPM reading during the measurements. The images were cropped to the region of interest (ROI) of 500×500 pixels and a pixel size of 19.5 µm, with the beam centered in the cropped region. The images were further smoothed using a median filter of 3 pixels. Lastly, for each quadrupole setting, the mean beam image was used for the reconstruction. Due to an disturbance in the measurement, only 22 out of the 30 quadrupole settings were correctly measured. The processed beam images are shown in Fig. 2.

Table 1: Results of the simulated beam matrix estimation. The target initial beam matrix is randomly varied from the design setting by 5%. We repeat the reconstruction 5 times to calculate the uncertainty.

Quantity	Target Val.	Reconst. Val.
β_x (m)	14.75	14.45 ± 0.09
α_x	3.41	3.34 ± 0.02
ϵ_x (nm)	77.25	76.28 ± 0.44
β_y (m)	2.97	2.94 ± 0.02
α_y	-0.465	-0.465 ± 0.001
ϵ_y (nm)	1.25	1.24 ± 0.01
η_x (m)	0.019	0.001 ± 0.013
$\eta_{x'}$	-0.019	-0.023 ± 0.003
σ_δ	9.26×10^{-4}	$9.29 \pm 0.06 \times 10^{-4}$

In the reconstruction, 10 000 macroparticles are tracked to simulate the beam images. The loss function is defined as the MSE between the simulated and the processed beam images. We used Adam optimizer [11] with a learning rate of 0.001 and 5000 steps. The fitting is repeated 5 times with slightly varied initial condition to estimate the uncertainty of the reconstruction process. As shown in Fig. 3, all 5 runs showed similar behavior and achieved comparable loss level. One set of the estimated initial beam matrix values are shown as dotted white ellipses in Fig. 2. The predicted beam images agree well with measured beam image, with the 1σ distribution shown as gray ellipses. The obtained beam parameters are shown in Table 2. In the real-world case the reconstructed values have orders of magnitude larger uncertainties compared to what is expected from the simulation result. The horizontal emittance is likely underestimated compared to the design setting. One possible reason is that the optimization task contains several local optima, which could produce similar beam images on the screen. This could be mitigated when all the 30 settings are correctly measured. The choice of the quadrupole strengths can also be optimized to fur-

ISBN: 978-3-95450-261-5 ISSN: 2673-7000 doi: 10.18429/JACoW-NAPAC2025-MOP093

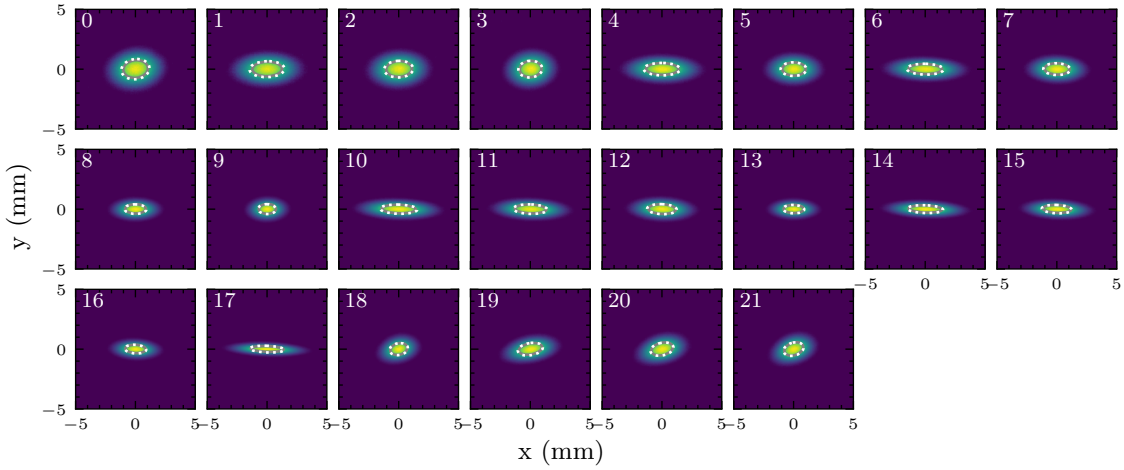

Figure 2: Measured beam on the diagnostic screen for 22 different sets of quadrupole settings. The images are averaged over 10 shots with backgrounds removed. The grey ellipses denote the beam profiles with 1σ widths, with the dotted white ellipses showing the simulated beam profiles with one set of the reconstructed initial beam matrix values.

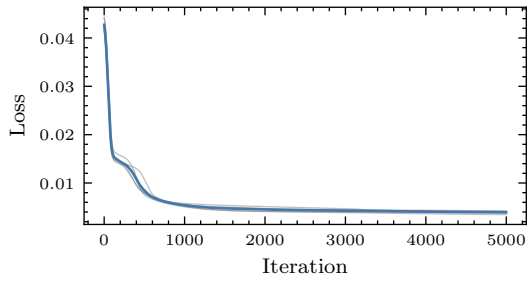

Figure 3: Loss values (mean squared error (MSE) between image pixel values) during the fitting process. Grey lines show the individual losses for 5 repeated runs and the blue line show the averaged loss.

ther increase the information gain of each observation, for example via Bayesian inference [12]. Another possible modification is to observe the beam at multiple screen locations. It needs to be noted that these uncertainties only represent the robustness of the reconstruction method, but it is unclear whether there are further systematic errors. To verify the reconstructed results, we would need either reference values from an independent method such as LOCO [13, 14] fitting of the booster lattice, or repeat the quadrupole scan measurement and compare the results from different runs [2].

On average, the fitting process took about 20 mins running on a NVIDIA A100 GPU. In addition, we tested fitting with 1000 macroparticles, which took about 15 mins on a personal laptop at the cost of slightly worse reconstruction result. Based on the processed beam images, it is possible to further speed up the process by reducing the size of ROI. The number of iterations can also be reduced by scheduling the learning rate. Overall, the computation time is at the same scale of the required measurement time, which takes about one hour for 30 quadrupole settings. In the future, we can expect to perform this reconstruction process online and use the result to inform the online control applications for accelerator operation.

Table 2: Results of the beam matrix estimated from measurement. The errors on the beam parameters are calculated over 5 reconstruction runs.

Quantity	Units	Meas. Val.
β_x	m	12.30 ± 1.19
α_x		2.28 ± 0.27
ϵ_x	nm	47.01 ± 4.97
β_y	m	2.13 ± 0.71
α_y		-0.58 ± 0.25
ϵ_y	nm	1.40 ± 0.37
η_x	m	-0.463 ± 0.063
$\eta_{x'}$		0.133 ± 0.027
σ_δ		$8.5 \pm 0.6 \times 10^{-4}$

CONCLUSION

We proposed a new approach to reconstruct the non-temporal components of the beam sigma matrix in a transport line by using differentiable simulation code Cheetah. This method shows promising result in the simulated environment on the new BTS lattice with strong chromatic aberrations. Applying the method on an initial real-world measurement produced larger uncertainties, which needs verification in future studies. The results are expected to be improved when including additional effects in the model such as the variable dispersion due to quadrupole offsets and magnet strength errors. The computation efficiency makes the method a promising candidate for online reconstruction of the beam properties during accelerator operation.

ACKNOWLEDGEMENT

We gratefully acknowledge the computing resources provided on Swing, a high-performance computing cluster operated by the Laboratory Computing Resource Center at Argonne National Laboratory.

ISBN: 978-3-95450-261-5 ISSN: 2673-7000 doi: 10.18429/JACoW-NAPAC2025-MOP093

REFERENCES

[1] A. Wolski, D. C. Christie, B. L. Militsyn, D. J. Scott, and H. Kockelbergh, "Transverse phase space characterization in an accelerator test facility", *Phys. Rev. Accel. Beams*, vol. 23, no. 3, p. 032 804, 2020. doi:10.1103/PhysRevAccelBeams.23.032804

[2] M. Borland, V. Sajaev, and K. Wootton, "Promise and challenges of a method for 5x5 sigma matrix measurement in a transport line", in *Proc. NAPAC'22*, Albuquerque, NM, USA, Aug. 2022, pp. 382–385. doi:10.18429/JACOW-NAPAC2022-TUPA18

[3] M. Borland, "ELEGANT: A flexible SDDS-compliant code for accelerator simulation", Argonne National Laboratory, Lemont, IL, USA, Tech. Rep. LS-287, 2000. doi:10.2172/761286

[4] J. Kaiser, C. Xu, A. Eichler, and A. Santamaria Garcia, "Bridging the gap between machine learning and particle accelerator physics with high-speed, differentiable simulations", *Phys. Rev. Accel. Beams*, vol. 27, no. 5, p. 054 601, 2024. doi:10.1103/PhysRevAccelBeams.27.054601

[5] R. Roussel *et al.*, "Advancements in backwards differentiable beam dynamics simulations for accelerator design, model calibration, and machine learning", in *Proc. LINAC'24*, Chicago, IL, USA, Aug. 24, pp. 768–771. doi:10.18429/JACOW-LINAC2024-THPB068

[6] D. Sagan, A. Coxe, G. Hoffstaetter, and M. Signorelli, "Bmad-Julia: A Julia environment for accelerator simulations including machine learning", in *Proc. IPAC'24*, Nashville, TN, USA, May 2024, pp. 2612–2615. doi:10.18429/JACOW-IPAC2024-WEPR52

[7] J. Wan, H. Alamprese, C. Ratcliff, J. Qiang, and Y. Hao, "JuTrack: A Julia package for auto-differentiable accelerator modeling and particle tracking", *Comput. Phys. Commun.*, vol. 309, p. 109 497, 2025. doi:10.1016/j.cpc.2024.109497

[8] R. Roussel *et al.*, "Phase space reconstruction from accelerator beam measurements using neural networks and differentiable simulations", *Phys. Rev. Lett.*, vol. 130, no. 14, p. 145 001, 2023. doi:10.1103/PhysRevLett.130.145001

[9] R. Roussel *et al.*, "Efficient six-dimensional phase space reconstructions from experimental measurements using generative machine learning", *Phys. Rev. Accel. Beams*, vol. 27, no. 9, p. 094 601, 2024. doi:10.1103/PhysRevAccelBeams.27.094601

[10] M. Borland, V. Sajaev, and Y. Sun, "Hybrid seven-bend-achromat lattice for the advanced photon source upgrade", in *Proc. IPAC'15*, Richmond, VA, USA, May 2015, p. TUPJE063. doi:10.18429/JACOW-IPAC2015-TUPJE063

[11] D. P. Kingma and J. Ba, "Adam: A method for stochastic optimization", in *Proc. ICLR'15*, San Diego, CA, USA, May 2015. doi:10.48550/arXiv.1412.6980

[12] U. von Toussaint, "Bayesian inference in physics", *Rev. Mod. Phys.*, vol. 83, no. 3, pp. 943–999, 2011. doi:10.1103/RevModPhys.83.943

[13] J. Safranek, "Experimental determination of storage ring optics using orbit response measurements", *Nucl. Instrum. Methods Phys. Res., Sect. A*, vol. 388, no. 1, pp. 27–36, 1997. doi:10.1016/S0168-9002(97)00309-4

[14] V. Sajaev and C. Yao, "Lattice measurements of the APS injector rings", in *Proc. IPAC'19*, Melbourne, Australia, May 2019, pp. 1619–1622. doi:10.18429/JACOW-IPAC2019-TUPGW091